



Role of typical pipes in disinfection chemistry within drinking water distribution system

Kai Ma , Xiazhen Jia, Hongda Han, Lin Zhao, Dongmei Fan, Jiankun Hu, Rong Li and Xiao Su

ABSTRACT

Deep insight into the forces driving chloramine decay in different pipe materials is the key to taking sound action to cope with pipe water quality deterioration. By using the newly developed RTCDM (refined Total Chloramine Decay Model) and pipe section reactor, the role of four typical pipes in disinfection chemistry was qualitatively and quantitatively compared, and the mechanism of pipe wall mediated chloramine decay was further described. As for the four typical pipes studied, the characteristics of deteriorating water quality, especially for accelerating total chloramine decay was in the order of cast iron pipe > steel pipe > cement lined ductile iron pipe > polypropylene-random pipe. Cast iron pipes, cement-lined ductile iron pipes, and steel pipes of long service age are characterized by one or two driving forces leading to TCR decay. Aged cast iron pipes could take up chloramine by Fe(0) and microbes (especially nitrifiers) spreading over the inner wall. Aged steel pipe is characterized by aggressive electrochemical corrosion and weak nitrification. Lime and gypsum leaching is the main cause, and nitrification/denitrification may also occur in aged cement-lined ductile iron pipe. Polypropylene-random pipes have a minimum effect on disinfection chemistry. This knowledge is of value in speculating the reasons leading to TCR loss in the full scale distribution system.

Key words | autodecomposition, disinfection chemistry, electrochemical corrosion, nitrification, total chloramine decay model

Kai Ma  (corresponding author)
Xiao Su
Tianjin Waterworks Group Co. Ltd,
Tianjin 300040,
China
E-mail: kaima1234@126.com

Kai Ma
Xiazhen Jia
Hongda Han
Jiankun Hu
Rong Li

Xiao Su
Tianjin Water Group Co. Ltd,
Tianjin 300042,
China

Kai Ma
Lin Zhao
Xiao Su

School of Environmental Science and Engineering,
Tianjin University,
Tianjin 300350,
China

Dongmei Fan
Qiqihaer City Longsha District Agricultural
Comprehensive Service Centre,
Qiqihaer 161005,
China

HIGHLIGHTS

- The developed RTCDM has good performance for predicting TCR decay in the bulk phase.
- The ability to accelerate TCR decay was in the order cast iron (CI) > steel > cement lined DI > polypropylene random copolymer (PPR).
- Chemical corrosion and nitrification are the main causes of TCR consumption for aged CI pipe.
- Aggressive corrosion and weak nitrification are the main causes of TCR lost for aged steel pipe.

INTRODUCTION

Distribution systems are the necessary infrastructure to deliver treated water to the terminal user. Except for frictional

head loss leading to hydraulic pressure decrease, pipes especially aged iron pipes, would also lead to water quality deterioration during long distance delivery, as complicated biochemical reactions occur within the pipe system. As water age increases within the 'biochemical reactor', the shift in water quality would be more significant compared with the treated water. Hence, stagnant water points or

This is an Open Access article distributed under the terms of the Creative Commons Attribution Licence (CC BY-NC-ND 4.0), which permits copying and redistribution for non-commercial purposes with no derivatives, provided the original work is properly cited (<http://creativecommons.org/licenses/by-nc-nd/4.0/>).

doi: 10.2166/ws.2020.376

end points of a distribution system are usually characterized by deteriorated water, e.g. red water, bacteria breeding, high turbidity, etc., which have always been the hotspot focused on by water utility and other authorities.

Many researchers have conducted a series of studies on disinfection chemistry to shed light on the cause and response strategy of negative effects of pipe walls. It was found that the biofilm attached to the pipe wall could accelerate chlorine-containing disinfectant decay (Lechevallier *et al.* 1988), if the water temperature is 15 °C or warmer, microbe activity would be further stimulated (Neden *et al.* 1992), which leads to serious microbial problems. Flow pattern is another factor that may result in greater biofilm formation under steady-state flow (Fish *et al.* 2017). Rittmann *et al.* (1989) found that nitrifiers developed in biofilms attached to pipe surfaces from the real distribution system. Moreover, Krishna *et al.* (2012) found that nitrifiers could release soluble microbial products (SMPs) to significantly accelerate chloramine decay. Recently, Herath & Sathasivan (2020) further confirmed that chloramine could force nitrifiers to produce, release, and accumulate chloramine decaying proteins (CDPs) to defend against disinfectant. As free ammonia produced from chloramine oxidation could stimulate nitrifier growth and metabolism (Janice 1993), a vicious circle would present eventually in the pipe system. It is widely accepted that once present in biofilms, nitrifiers can hardly be eliminated by merely increasing the chloramine concentration of treated water (Woolschlager *et al.* 2005; Ma *et al.* 2020). Consequently, periodic free chlorine disinfection and reducing free ammonia levels are recommended and taken as the nitrification control strategy.

Another driving force that may accelerate disinfectant decay is electrochemical corrosion that occurs in unlined cast iron, galvanized iron, and steel pipes. Chlorine/chloramine are all strong oxidants with standard electrode potentials significantly higher than Fe(0), which makes chlorine/chloramine-mediated corrosion commonly occur in the distribution system. In addition to disinfectant, the exact corrosion process is dependent on flow characteristics and water quality, e.g., Cl⁻, DO, SO₄²⁻, pH, alkalinity. Among them, increase in Cl⁻, DO, SO₄²⁻ could lead to higher corrosion rates (Pisigan and Singley 1985). By conducting a two year pilot study, Imran *et al.* (2005) found that alkalinity, Cl⁻, SO₄²⁻, sodium, and DO of the source

water or blend of source waters had a significant effect on release of corrosion by-products in the form of red water, temperature and hydraulic retention time were the significant physical and operational parameters. Recently, Li *et al.* (2014) proved that α -FeOOH was the main corrosion product for both chlorine- and chloramine-disinfection systems, whereas much denser crystallized particles were formed in drinking water distribution systems (DWDSs) with chloramine. This characteristic may prevent further corrosion within the downstream iron pipes for the chloramine-disinfection system. However, it is necessary to keep in mind that, accompanied by electrochemical corrosion, a series of shifts in water quality (increase in pH, alkalinity, Fe residual) happens as well, which may lead to water quality deterioration. Analysis and summary of these data could help us to make an adverse inference on the reason for the disinfectant fast decay and water quality degeneration.

Many mechanism studies have been conducted at the laboratory scale under delicately controlled conditions. In a full-scale distribution system, a delivery path consists of many sections of pipes with different diameters and materials. As a result, the disinfectant decay is caused by a variety of factors, including microorganism-mediated consumption and electrochemical corrosion. Researchers have been focusing on the effects of certain pipe materials on disinfectant decay speed by constructing suitable physical models. Digiano & Zhang (2005) developed the pipe section reactor (PSR) to quantify 'wall demand' chlorine decay rate, and found that higher velocity, lower pH, and lower DO could promote chlorine decay for old cast iron pipes. By using the same reactor, Westbrook & Digiano (2009) found the chloramine decay rate was much slower for cement-lined ductile iron pipe than it was for tuberculated cast iron pipes. Another field study reported that unlined cast iron pipes had the largest chlorine decay rate relative to unlined ductile iron pipes and PVC pipes (Huang & McBean 2008). Lately, Zhang *et al.* (2017) developed a model full-scale water distribution system to examine the effects of pipe materials on chlorine decay, and found that stainless steel pipes had the largest decay rate, followed by cement-lined ductile iron pipes, and polyethylene (PE) pipes. Even the relationship between water quality indices and disinfectant decay rate were deeply explored, but this failed to establish the relationship between the exact driving forces (e.g., biofilm

consumption, corrosion) and the decay process, which makes the diagnosis on fast disinfectant decay ineffective. So it was suggested to explore the exact biochemical/physico-chemical forces embedded in different pipes by analyzing water quality variations simultaneously.

Other than experimental study, model calculation is another effective method, and has always been a way for improvement since the 1950s. Data-based empirical models and mechanistic models are the two major types of models capable of giving total chlorine residuals at key locations in the distribution system with certain travel time. The empirical model is developed based on historical data, and could reflect the differences in disinfectant decay coefficient under certain conditions, e.g. the difference caused by the pipe material (Westbrook & Digiano 2009). However, when environmental conditions change even in an invisible manner, the prediction accuracy may be not high enough to be used in the distribution system. The mechanistic/semi-empirical model includes the previous research findings on reaction processes of interest, which could gradually 'squeeze out' prediction uncertainties in the course of improvement of the mechanistic model. Hence if the key reaction processes could be described in the mechanistic/semi-empirical model, the model calculation could assist administrators to select proper disinfection strategies by presenting quantifiable modelling results.

Characterizing the disinfection chemistry for different pipes is essential to obtain a deep insight into the full-scale distribution system. To achieve this, we developed new type PSR (Figure S2, supplementary material), which was used to study the influence of five pipes on drinking water quality. Secondly, to quantify pipe wall consumption, the wall decay rate was calculated by using the refined Total Chloramine Decay Model (TCDM). Finally, the characteristic driving forces were inferred for the four typical pipes by analyzing the variations in water quality indices. Based on which, the diagnostic method was put forward to find the reasons for pipeline water quality deterioration.

MODEL CONSTRUCTION

Chloramine, as an active reagent, could participate in many biochemical reactions in distribution systems. Based on

extensive study of disinfection chemistry, chloramine decay could be basically ascribed to the autodecomposition and oxidizing reductive compounds in bulk phase, and to the consumption induced by the pipe wall. Specifically, the autodecomposition model could be described by 19 reactions, whose kinetic and thermodynamic coefficients have been calibrated and validated for different pH and temperature conditions (Vikesland *et al.* 2001; Huang & McBean 2008; Ricca *et al.* 2019). The oxidizing reactions in the bulk phase are commonly related to natural organic matter (NOM), which is often found in source water. The oxidation of NOM by chloramine and chlorine was described as a biphasic second-order kinetic model relating TOC with four specific reaction parameters (Duirk *et al.* 2005). The above two components have been packaged in one prediction model to simulate drinking water chloramine formation and decay in a batch reactor (Wahman 2018), the chloramine decay model and corresponding reaction rates for the above two components are described in Ricca *et al.* (2019) and Wahman (2018). While, nitrite could also be oxidized by chloramine in bulk phase (Margerum *et al.* 1994), and the pipe wall-induced chloramine decay accounts for much of the overall loss (Rossman *et al.* 1994; Huang & McBean 2008). Hence we incorporated a nitrite oxidation component and pipe wall consumption component into the prediction model to generate the TCDM in our previous study. The chloramine decay model and corresponding reaction rates relating nitrite and pipe wall are given in Tables 1 and 2, respectively. The TCDM has shown its ability to give a reasonable explanation for the fast decay of the total chlorine residual (TCR) in a real distribution system (Ma *et al.* 2020).

Recently, we found the inability of TCDM in predicting the TCR for bulk phase decay experiments under different conditions, which could be seen in Figure S1 (supplementary material). The stark contrast of prediction results (dotted line in Figure S1) to the experimental data (solid block in Figure S1) manifested the insensitivity of TCDM to physico-chemical factors. As for aqueous solution, chloramine concentration is in chemical equilibrium with that of chlorine. Chlorine also experiences autodecomposition to produce ClO_3^- or O_2 , which was proved to be temperature, pH, and $\text{NH}_4^+\text{-N}$ dependent (Adam *et al.* 1992; Adam & Gordon 1998). Hence, we added the hydrolysis reaction of monochloramine to hypochlorous acid (see No. 1 in Tables 1 and 2), and

Table 1 | Chlorine autodecomposition model and chloramine decay model related to nitrite oxidation and pipe wall consumption

No.	Reaction stoichiometry	Rate coefficient/equilibrium constant	Reference
1	$\text{NH}_2\text{Cl} + \text{H}_2\text{O} \rightarrow \text{HOCl} + \text{NH}_3$	$k_1 = 3.792 \times \exp(-1,510/T) \times 10^{0.000118 \times T - 0.0786 \times T + 15.5} \text{ M}^{-1} \text{ h}^{-1}$	Adjusted from Corbett <i>et al.</i> (1953) and Morris & Isaac (1983)
2	$2\text{HClO} + \text{ClO}^- \rightarrow \text{ClO}_3^- + 2\text{H}^+ + 2\text{Cl}^-$	$k_2 = 2.1179 \times 10^{15} \times \exp(-48,345/8.314/T) \text{ M}^{-1} \text{ h}^{-1}$	Adam <i>et al.</i> (1992)
3	$2\text{ClO}^- \rightarrow \text{O}_2 + 2\text{Cl}^-$	$k_3 = \exp(-9.24/8.314 + \log(T) + 24.76) \times \exp(-129400/8.314/T) \text{ M}^{-1} \text{ h}^{-1}$	Church (1994)
4	$\text{OCl}^- + \text{NO}_2^- + \text{H}^+ \rightarrow \text{NO}_3^- + \text{Cl}^- + \text{H}^+$	$k_4 = 5.04 \times 10^{15}$	Margerum <i>et al.</i> (1994)
5	$\text{NH}_2\text{Cl} + \text{Pipe wall} \rightarrow \text{Productions}$	k_{wall}	Westbrook & Digiano (2009)

Table 2 | Reactions and rates for chlorine autodecomposition model and chloramine decay model related to nitrite oxidation and pipe wall consumption

No.	Reaction	Rate
1	$\text{NH}_2\text{Cl} + \text{H}_2\text{O} \rightarrow \text{HOCl} + \text{NH}_3$	$a_1 = k_1 \times [\text{NH}_2\text{Cl}]$
2	$2\text{HClO} + \text{ClO}^- \rightarrow \text{ClO}_3^- + 2\text{H}^+ + 2\text{Cl}^-$	$a_2 = k_2 \times [\text{ClO}^-] \times [\text{ClO}^-] \times [\text{HClO}]$
3	$2\text{ClO}^- \rightarrow \text{O}_2 + 2\text{Cl}^-$	$a_3 = k_3 \times [\text{ClO}^-] \times [\text{ClO}^-]$
4	$\text{OCl}^- + \text{NO}_2^- + \text{H}^+ \rightarrow \text{NO}_3^- + \text{Cl}^- + \text{H}^+$	$a_4 = k_4 \times [\text{NO}_2^-] \times [\text{OCl}^-] \times [\text{H}^+]$
5	$\text{NH}_2\text{Cl} + \text{Pipe wall} \rightarrow \text{Production}$	$a_{\text{wall}} = k_{\text{wall}} \times [\text{NH}_2\text{Cl}]$

further incorporated an chlorine autodecomposition model into the original TCDM model (see Nos. 2 and 3 in Tables 1 and 2), to better describe the chlorine-containing disinfectant decay process. The refined TCDM (RTCDM), consisting of 23 differential equations for kinetic reactions and four algebraic equations for equilibrium reactions, was edited in C programming language on MATLAB software (version R2018b), and solved using differential algebraic equations (DAE) solver ode15s. Finally, The RTCDM showed an excellent ability in predicting the experimental data as shown in Figure S1.

The calculation studies, based on the Nonlinear Least Square Approximation Method, were carried out on five sets of water quality data from pipe section experiments using RTCDM, and that from bulk phase decay experiment using a first-order kinetic model. The curve fitting calculation would stop only until the size of the gradient was less than the value of the optimality tolerance. Consequently, k_{wall} or k_b was obtained as the output parameter. The contribution of pipe wall-induced decay could be observed by comparing the k_{wall} from the pipe section

experiments and the k_b from the bulk phase decay experiment under the same ambient conditions.

MATERIALS AND METHODS

Bulk decay experiment

To confirm the necessity of including a chlorine autodecomposition model in the TCDM, firstly we filled two 4 L brown glass bottles with feed water, and put them in water bath at 8 °C and 16 °C, respectively. The samples were collected at the operation time of 0, 1, 2, 4, 8, 24, 48, 72 h. TCR, pH, turbidity, water temperature, $\text{NH}_4^+\text{-N}$, and $\text{NO}_2^-\text{-N}$ were determined for each sample. Furthermore, to isolate the pipe wall consumption from TCR overall decay, another bulk decay experiment was conducted in a water bath at 25 °C identical to the pipe section experiments. Samples at 0, 1, 2, 4, 8, 24, 48, 72 h were collected to perform TCR measurements only.

Pipe section experiments

To differentiate the contribution of the pipe wall from the disinfectant overall decay, we constructed the continuous flow PSR, which is capable of quantifying decay coefficients induced by different kinds of pipes. The reactor mainly consisted of a PLC controller, infinitely variable speed fluid propeller, intelligent flowmeter, water-bath heating system, and pipe fixator (as shown in Figure 1). The flow rate of feed water could be controlled within the range 0–1.5 $\text{m}^3 \cdot \text{h}^{-1}$, the water temperature could be maintained with an error of ± 0.5 °C. What is more, pipe sections to be tested, with

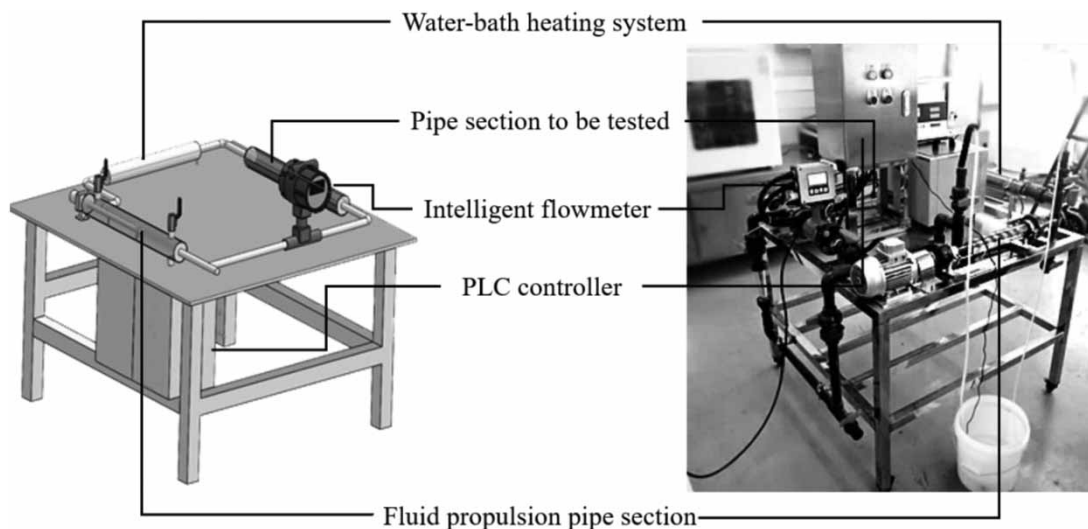


Figure 1 | Schematic of pipe section reactor.

diameter ϕ ranging from 1 to 10 cm, could be flexibly replaced and fixed on the reactor using a pipe fixator.

For the newly fabricated reactor, pure water was pumped to flush the pipe system for 7 days with a polymethyl methacrylate pipe fixed on the reactor. Afterwards the water containing $10 \text{ mg}\cdot\text{L}^{-1}$ Cl (NaClO solution) was pumped to disinfect the system for 2 days. At the end, pure water was pumped to rinse the system for 2 hours. As polymethyl methacrylate is inert to Cl-containing disinfectants, the corresponding pipe section was selected as the basic tube. The other four pipe sections with different materials, diameters, and ages, were replaced to determine their contributions to the total chlorine residual decay separately. The characteristics of the five pipe sections used in the study are shown in Table 3.

For every formal experiment, tap water with TCR of $0.8\text{--}1.2 \text{ mg}\cdot\text{L}^{-1}$ was pumped into the system. In the meantime, the water-bath heating system and fluid propeller were started to maintain the fluid temperature of $25 \pm 0.5 \text{ }^\circ\text{C}$ and

flow velocity of $0.22 \text{ m}\cdot\text{s}^{-1}$ (except for CL-DI pipe and steel pipe). The time was set as the start point when the air bubble was completely excluded from the vent. The samples were collected at the operation times of 0, 1, 4, 8, 24, 48, and 72 h. TCR, pH, turbidity, water temperature, three forms of inorganic nitrogen, and iron residual were measured. As CI pipe and steel pipe were reported to have microbes- or corrosion tuberculation-mediated contributions to the TCR decay (Digiano & Zhang 2005; Hua et al. 2011; Li et al. 2014), the pipe sections occupied here were installed and tested in the order PMMA pipe, PPR pipe, CL-DI pipe, steel pipe, CI pipe. In addition, the system was flushed with pure water for 24 h between the two neighboring formal experiments, to minimize the effects induced by the former pipe.

Feed water preparation and analytical methods

The institutional tap water with water age of 10 h was collected as the feed water. The collecting tap was a regularly

Table 3 | Characters of pipes used in the study

Material	Abbreviation	Diameter/mm	Length/mm	Age of pipe
Polymethyl methacrylate pipe	PMMA pipe	30	500	Newly purchased
Polypropylene-random pipe	PPR pipe	30	500	Newly purchased
Cement lined ductile iron pipe	CL-DI pipe	100	500	~20 yrs
Steel pipe	Steel pipe	100	500	~20 yrs
Cast iron pipe	CI pipe	19	500	~20 yrs

used one, without influence from any water filtration, softening or heating device. After initial draw out for 18 minutes, and then flushing the container for 2 minutes, about 20 L tap water was collected for each of the five formal experiments. The physico-chemical properties of feed water varied within the experimental period. The properties of the feed water could be seen in Table 4. TCR was measured by the *N,N*-diethyl-*p*-phenylenediamine (DPD) method with a portable colorimeter (DR300, HACH, USA). Turbidity and pH were tested by turbidity meter (TU5200, HACH, USA) and pH meter (S210-K, METTLER TOLEDO, Switzerland) respectively. Total alkalinity was determined by acid–base indicator titration method according to Water and Wastewater Monitoring Analysis Method. Using a UV–Visible spectrophotometer (DR6000, HACH, USA), $\text{NH}_4^+\text{-N}$ was determined by salicylate method at the wavelength of 655 nm with resolution of $0.01 \text{ mg}\cdot\text{L}^{-1}$, $\text{NO}_2^-\text{-N}$ was determined by the diazotization method at the wavelength of 507 nm with a resolution of $0.001 \text{ mg}\cdot\text{L}^{-1}$, $\text{NO}_3^-\text{-N}$ was determined by the Cd reduction method at the wavelength of 507 nm with a resolution of $0.01 \text{ mg}\cdot\text{L}^{-1}$, iron residual was determined by 1,10-phenanthroline method at the wavelength of 510 nm with a resolution of $0.01 \text{ mg}\cdot\text{L}^{-1}$. TOC was determined by the TC-IC method using a TOC analyzer (TOC-L, Shimadzu, Japan).

Data input strategy

As well as comparative analysis, the water quality data were also used for calculation studies by inputting the data into the

RTCDM. The data of the seven parameters (listed in Table 4 except $\text{NO}_3^-\text{-N}$, Fe residual, and turbidity) at the time of 0 h were set as the initial conditions. The time series data of TCR for each formal experiment were set as the fitting target value. Upon model calculations, the differences in the pipes sections could be totally reflected from the perspective of reshaping the decay dynamics of disinfectant.

RESULTS AND DISCUSSION

Weak effect of PMMA pipe on drinking water quality

Prior to the four pipes commonly used in the distribution system, PMMA's effect on chloramine decay was studied by installing PMMA pipe onto the PSR. Figure 2 shows the variations in TCR, pH, and turbidity of the pipe water with time. Both pH and turbidity varied within a small range of 7.92 – 8.02, and 0.184 – 0.271 NTU, respectively, which means minimum effect of PMMA pipe wall on drinking water. However, as compared with the bulk decay within the brown glass bottle (Figure S5), TCR was characterized by a faster decay, descending from 0.96 to $0.05 \text{ mg}\cdot\text{L}^{-1}$. In other words, even in the 'clean' pipe system, the treated water would experience fast TCR decay within 1 day to the level lower than limit ($0.05 \text{ mg}\cdot\text{L}^{-1}$ total chlorine) specified by Chinese Standard for Drinking Water Quality.

The PSR employed here consisted of non-uniformed pipes, which produces local turbulence within the system.

Table 4 | Properties of feed water used in the study

Parameters	Value
Temperature ($^{\circ}\text{C}$)	14–23.9
TCR ($\text{mg}\cdot\text{L}^{-1}$)	0.76–1.24
pH	7.81–8.05
Alkalinity ($\text{mg}\cdot\text{L}^{-1}$)	95–105
Turbidity (NTU)	0.290–0.328
$\text{NH}_4^+\text{-N}$ ($\text{mg}\cdot\text{L}^{-1}$)	0.22–0.29
$\text{NO}_2^-\text{-N}$ ($\text{mg}\cdot\text{L}^{-1}$)	0.003–0.055
$\text{NO}_3^-\text{-N}$ ($\text{mg}\cdot\text{L}^{-1}$)	0.04–0.40
Fe residual ($\text{mg}\cdot\text{L}^{-1}$)	<0.05–0.06
TOC ($\text{mg}\cdot\text{L}^{-1}$)	1.0–1.5

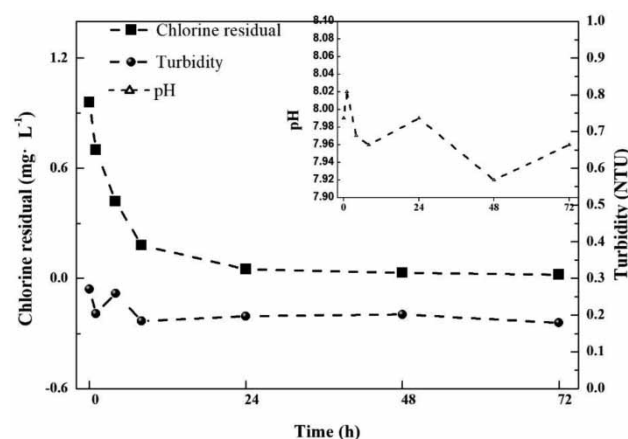


Figure 2 | Variations in TCR, pH, and turbidity in the PMMA pipe system.

Water flow, especially for the turbulence would accelerate the mass transfer of the highly active molecule (mainly monochloramine) from the bulk phase to the pipe wall (Rossman *et al.* 1994; Westbrook & Digiano 2009). Furthermore, the small ϕ pipes employed here is characterized by a small cross-section area–perimeter ratio, the pipe wall effects would be more magnified relative to the large ϕ pipes. Even so, the TCR decay was obviously slower than that in the four typical pipe systems as stated here. Hence, PMMA pipe was selected as the ideal basic pipe to have a weak effect on drinking water quality.

Role of typical pipes in disinfection chemistry

Figure 3 presents the TCR decay process of the five pipe systems. As shown in Figure 3, the pipe section-mediated TCR decay difference could be visually discriminated by comparing the curvature radius of the trendlines within the time span of 0–24 h. Among the five pipes, the PMMA pipe had the minimum effect on TCR decay, followed by the PPR pipe, CL-DI pipe, steel pipe, and CI pipe could markedly accelerate TCR decay at the fastest speed. The order of chloramine decay rate in our study was identical to that for chlorine reported by Zhang *et al.* (2017). Another study on chloramine decay also found that the CI pipe had higher decay rate than CL-DI pipe (Westbrook & Digiano 2009). Here, the direct comparison of pipe-mediated chloramine decay was presented for the four commonly used pipes

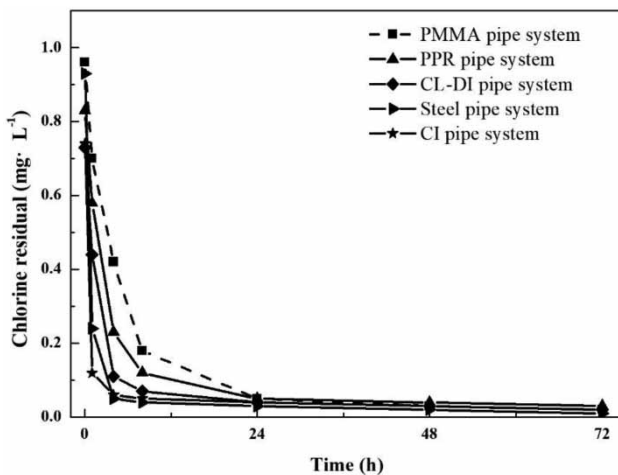
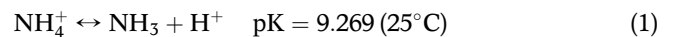


Figure 3 | Comparison of total chlorine decay within different pipe systems.

in the distribution system simultaneously, and the quantified contribution stemmed from the pipe wall is further described in this paper.

Figure 4 shows the variations in pH with time for the five pipe systems. The water from PMMA pipe system (dashed line in Figure 4) had the smallest pH changes during the experimental period. As for the PPR pipe system, after the small vibration within the first 4 h, the pipe water experienced slow pH descending to 7.87 at 72 h, which may be caused by leaching of acidic organic matter to the bulk phase (Zhang *et al.* 2014). The pH changing behaviors for CL-DI, and CI pipe system were completely different from the former two, and had the feature of ascending to the peak for the first 24 h, and then descending continuously. The CL-DI pipe system had the largest changing range of 8.00–8.87, leaching of lime from the cement matrix is responsible for the initial elevation (Douglas *et al.* 1996), which may break the biochemical equilibrium of the downstream pipe water. More importantly, the obvious elevation in pH would convert $\text{NH}_4^+\text{-N}$ to $\text{NH}_3\text{-H}_2\text{O}$ (see Equation (1)), and further release NH_3 (g), which may accelerate the autodecomposition of chloramine because of higher $\text{Cl}_2\text{:NH}_4^+\text{-N}$ ratio (Huang 2008):



The CI pipe could also stimulate pH to increase, but with smaller amplitude, followed by the steel pipe. As for the two pipes, zero-valent iron pipes are exposed to

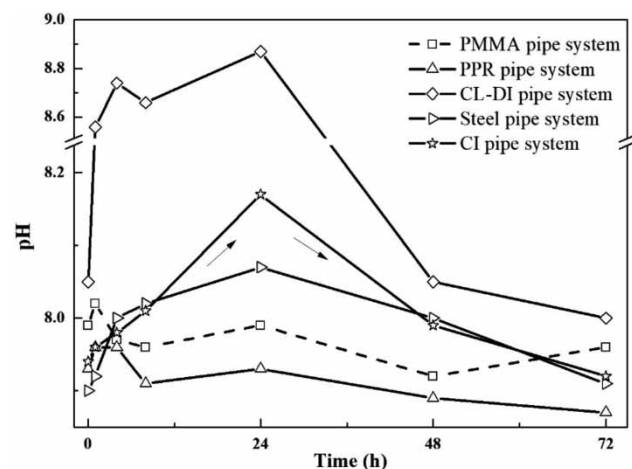


Figure 4 | Variations in pH within different pipe systems.

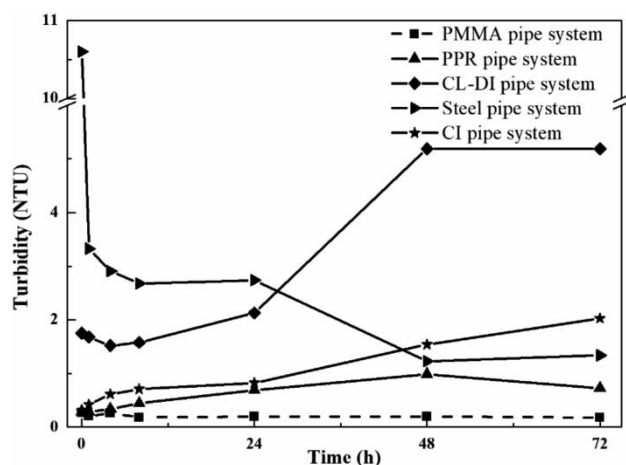
Table 5 | Standard electrode potentials pertinent to the zero-valent iron corrosion in basic solutions^a

Redox couple	Half-reaction	Standard electrode potential/V
Cl(I)/Cl(-I)	$\text{ClO}^- + \text{H}_2\text{O} + 2\text{e}^- = \text{Cl}^- + 2\text{OH}^-$	0.841
O(0)/O(-II)	$\text{O}_2 + 2\text{H}_2\text{O} + 4\text{e}^- = 4\text{OH}^-$	0.401
N(V)/N(III)	$\text{NO}_3^- + \text{H}_2\text{O} + 2\text{e}^- = \text{NO}_2^- + 2\text{OH}^-$	0.01
Fe(II)/Fe(0)	$\text{Fe}^{2+} + 2\text{e}^- = \text{Fe}$	-0.44

^aReferenced to Lange's Handbook of Chemistry, 13th edition (Dean 1985).

chloraminated water, and could be oxidized by three oxidants popular in drinking water. Given standard electrode potentials (shown in Table 5), the conditional potentials (E) are about 0.946 – 0.956, 0.755 – 0.762, and 0.021 – 0.402 V for ClO^- , O_2 , and NO_3^- respectively, according to the Nernst Equation under our physico-chemical conditions listed in Table 4. The conditional potential (E) of Fe is lower than -0.617 V, which is obviously smaller than those of the oxidants. Hence, corrosive reactions could aggressively occur at the initial phase, accompanied by which, the pH would also ascend as OH^- forms continuously. Interestingly, the pH of the three pipe systems uniformly decreased after the 24 h operation. The cause could be tentatively deduced by comprehensive analysis of the changes in three forms of inorganic nitrogen (see Part Figure).

Figure 5 shows the impact of different pipes on water turbidity. The Water turbidity was always at the low level continuously along the experimental period for the PMMA pipe system (dashed line in Figure 5). As for the PPR pipe system,

**Figure 5** | Variations in turbidity within different pipe systems.

the water turbidity showed elevation and deviated from the value of the PMMA pipe after an 8 h operation, which proved the cumulative effect of PPR pipe on water quality during delivery. In contrast, CL-DI and steel pipe systems were characterized by higher initial value at 0 h, which was caused by denudation of corrosion debris that was loosely attached on the surface of the steel pipe wall, or leaching of lime from the CL-DI pipe when injecting the feed water into the system. However, when the flow regime became stable, the difference of the two pipes could be seen. As the CL-DI pipe was constantly flushed by fresh water, leached lime and gypsum would accumulate in the bulk phase (see Figure S3), water turbidity rose continually to the final value of 5.19 NTU, which was far beyond the limit (1 NTU total chlorine) specified by Chinese Standard for Drinking Water Quality.

At the flow velocity of $0.10 \text{ m}\cdot\text{s}^{-1}$, the water turbidity in the steel pipe system went down from 10.6 to 1.34 NTU, and iron residual decreased from 0.26 to $0.10 \text{ mg}\cdot\text{L}^{-1}$, which reminds us to be aware of the sedimentation of corrosion debris downstream. By contrast with steel pipe, CI pipe with a long service age has dense crystallized particles on the surface (Li *et al.* 2014), the water turbidity increased gradually from 0.306 to 2.03 NTU within the experimental period of 72 h, and may further elevate as water age increases. As a whole, the four pipes exerted the ability for deteriorating water quality, especially for accelerating TCR decay in the order of the CI pipe > steel pipe > CL-DI pipe > PPR pipe. The parameters of pH and turbidity reflected a similar changing order except for the CL-DI pipe, as the leaching effect has surpassed microbe- or corrosion-mediated effects that occurred on the pipe surface.

Quantification of pipe wall effect

A first order kinetic model was used to fit the bulk decay data (under 25°C) with k_b to be calibrated. The fitting line could represent the experimental data with little error (see Figure S4). The calibrated parameters could be seen in Table 6. The first order kinetic model gave the k_b $0.018 \pm 0.005 \text{ h}^{-1}$ with acceptable goodness of fit. The k_b , within the two recently reported values (Krishna *et al.* 2012; Ma *et al.* 2020), is used as the reference value relative to k_{wall} obtained from RTCDM for pipe section experiments.

Table 6 | Summary of wall decay coefficient obtained from RTCDM calibrations

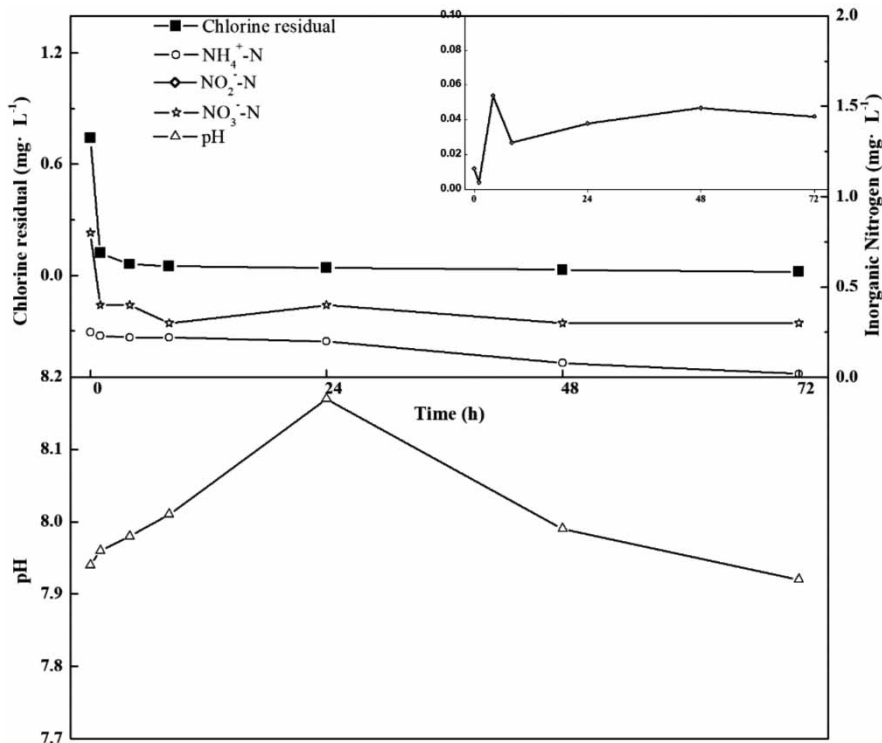
Material	Goodness of fit	k_b (h^{-1}) ^a	k_{wall} (h^{-1})	k_{wall}/k_b
PMMA	0.9884	0.018 ± 0.005	0.211	11.7
PPR	0.9849		0.308	17.1
CL-DI	0.9853		0.479	26.6
Steel	0.9920		1.297	72.0
CI	0.9784		1.679	93.3

^aThe goodness of fit for bulk decay data (under 25 °C) is 0.968.

To further quantitatively compare the five pipes, the time series data of TCR were input into RTCDM to conduct fitting calculations. Fitting lines with corresponding experimental data of the five pipes are shown in Figure S5. Besides visually good fitting results, the calibrated parameters are tabulated in Table 6. The RTCDM could well represent the experimental data as goodness of fit was uniformly larger than 0.97. The calibrated k_{wall} was all larger than 0.2 h^{-1} , which is obviously larger than two reported value ($<0.075 \text{ h}^{-1}$) obtained from field studies (Kulkarni *et al.* 2018; Ma *et al.* 2020), but is comparable with another

laboratory experimental result ($0.149 - 0.177 \text{ h}^{-1}$) (Westbrook & Digiano 2009). Kulkarni *et al.* (2018) found that chloramine decay rate for the downstream pipeline was larger relative to the upstream pipeline. So, the k_{wall} in the field study would be the mean value averaged for ‘clean’ pipes and ‘dirty’ pipes. Furthermore, pipes in the real distribution system had a large cross-section area-perimeter ratio, which makes the pipe wall-induced TCR decay less significant than that in the pipe section study. For these reasons, PSR could greatly magnify the pipe wall-induced effects on drinking water quality.

The k_{wall}/k_b ratio (see the last column in Table 6) reflects the relative contributions of bulk decay and pipe wall consumption to the overall decay. Even for the PMMA pipe, the persistent consumption of wall demand was 11.7 times stronger than the bulk decay. The largest one was 93.3 for the CI pipe system. This is powerful evidence for a more prominent effect of pipe wall over bulk decay. Finally, the pipe wall consumption intensity for the five pipes could be compared by reading k_{wall} listed in Table 6. The k_{wall} increased in the order of PMMA pipe, PPR pipe, CL-DI pipe, steel

**Figure 6** | Variations in water quality within the CI pipe system. Inset shows the changes in NO_2^- -N concentration with time.

pipe, and CI pipe from 0.211 to 1.679 h⁻¹, which further confirms the deduction obtained from Figure 3.

Mechanism of pipe wall-mediated chloramine decay

It is broadly reported that pipe wall-mediated disinfectant decay can be caused by electrochemical corrosion, microbe nitrification, and leaching, which could be identified by the changes in regular water quality indices (Woolschlager *et al.* 2005; Zhang *et al.* 2008; Pressman *et al.* 2012; Li *et al.* 2014). Accordingly, the coordinated variations in water quality indices were tabulated in Table S1 (supplementary material). It is convenient to diagnose the problem relating to pipes by referring to Table S1, just like pathogenic diagnosis according to blood test results.

Figure 6 presents the variations in TCR, NH₄⁺-N, NO₂⁻-N, NO₃⁻-N, and pH with time for the CI pipe experiment. As for the aged CI pipe, ionic tuberculation spread almost all over the inner surface. The fast decline in NO₃⁻-N, and elevation in pH and NO₂⁻-N manifested the corrosion reaction as the zero-valent iron acts as the reductant (see Table 5). Biofilms

with physiological heterogeneity may also become attached to the surface of the pipe wall (Lewandowski & Beyenal 2005). The continuous decline in NH₄⁺-N to 0.02 mg·L⁻¹ and fast decrease in pH are the clear indications that nitrification occurred in the pipe section system, which was further confirmed by the maintenance of >0.04 mg·L⁻¹ NO₂⁻-N within the last 2 days (Zhang *et al.* 2009; Liu *et al.* 2020). The gradual decline in NH₄⁺-N may be caused by microbe adaptation to the flow regime changes from standing water (microbe cultivation before pipe section experiment) to flow water (formal experiment). Meanwhile, the denitrification even for 2–6 mg·L⁻¹ DO (Liu *et al.* 2020), and persistent electrochemical corrosion can dominate the NO₃⁻-N at low levels in the later period. As a whole, the main driving forces for the chloramine decay are electrochemical corrosion, and microbe nitrification in the aged CI pipe lines.

Figure 7 shows the variations in water quality with time for the steel pipe experiment. NO₃⁻-N stayed at a constant level, while pH kept increasing within the first 8 h, which was caused by the redox reaction between HClO/NH₂Cl or O₂ and Fe. The subsequent decline of NO₃⁻-N and elevation of

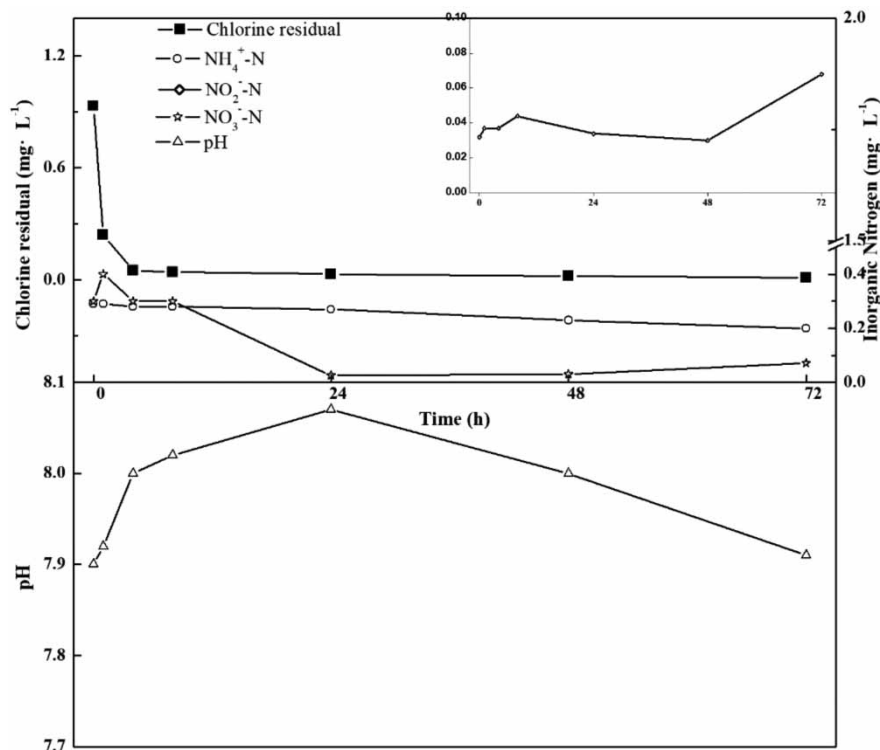


Figure 7 | Variations in water quality within the steel pipe system. Inset shows the changes in NO₂⁻-N concentration with time.

pH proved that NO_3^- -N participated in the corrosion reaction. Compared to CI pipe, NH_4^+ -N levels decreased at a slower speed for steel pipe, meanwhile pH decreased after 24 h of operation, which is the evidence that nitrification occurred in the steel pipe system, but was still weaker than that for the CI pipe. Furthermore, the elevation of NO_2^- -N to $0.068 \text{ mg}\cdot\text{L}^{-1}$ at 72 h and the gentle rise of NO_3^- -N after 24 h confirmed the microbial action of ammonia oxidizing bacteria (AOB) and nitrite oxidizing bacteria (NOB), respectively. Therefore, aged steel pipe could stimulate chloramine decay through aggressive electrochemical corrosion, accompanied by the nitrification weaker than in the aged CI pipe.

Figure 8 depicts the variations in water quality with time for the CL-DI pipe experiment. Because of cement dissolution, pH ascended sharply from 8.05 to 8.74 within the first 4 h and, as a result, NH_4^+ -N decreased to a low level, while NO_2^- -N and NO_3^- -N did not change obviously. It has been found that NO_2^- -N and NO_3^- -N could be reduced by denitrifiers at pH ranging from 6.5 to 9.0 with maximum NO_3^- -N reduction rate at pH 8.0 (Pan *et al.* 2012). Peng *et al.* (2006) reported that denitrification could change water pH, and result in pH

increase with a peak higher than 8.6 at the early stage, then make pH decrease after the 'nitrate/nitrite apex'. The synchronized decline of NH_4^+ -N, NO_2^- -N, NO_3^- -N, and pH could be explained by the simultaneous occurrence of nitrification and denitrification within the pipe section system. In brief, lime and gypsum leaching is the main cause that affects the drinking water disinfection chemistry for the CL-DI pipe, and nitrification and denitrification may occur within the CL-DI pipe delivering aged water continuously.

Figure 9 shows the variations in water quality with time for the PPR pipe experiment. Even the PPR pipe has some effect on water turbidity there was no significant impact of the pipe on water chemical indices as reflected by the small variations in pH of 0.1 unit, NH_4^+ -N of $0.06 \text{ mg}\cdot\text{L}^{-1}$, NO_2^- -N of $0.004 \text{ mg}\cdot\text{L}^{-1}$, respectively. The reason for the fluctuation in NO_3^- -N within the first 24 h is still not clear, and need to be further studied. Therefore, it is reasonable to use the PPR pipe as drinking water delivery pipes under suitable ambient conditions as there was minimum impact on water quality compared with the other three typical pipes employed in our study.

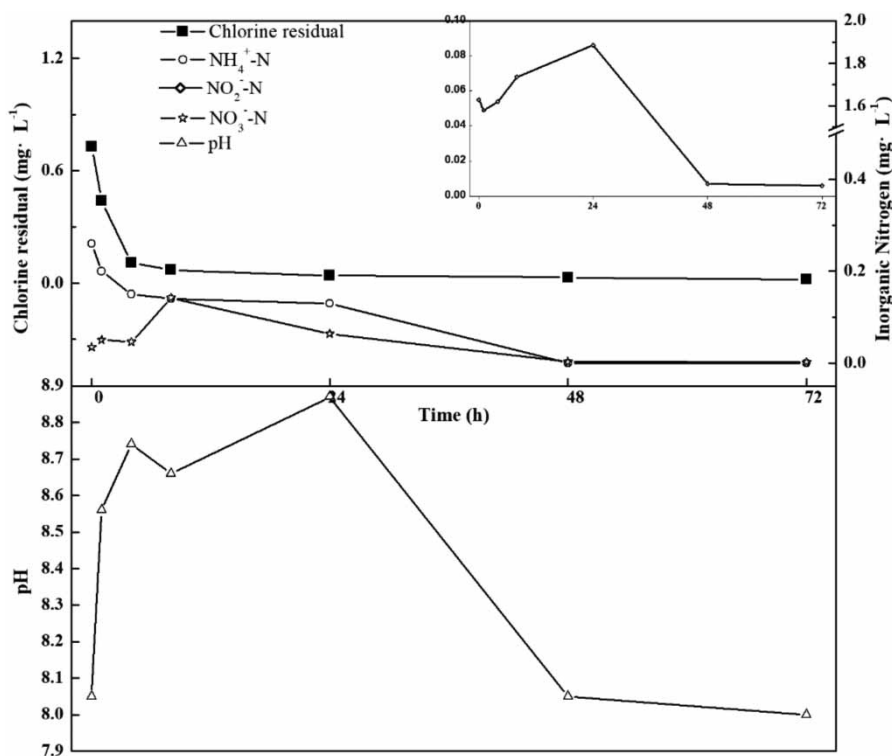


Figure 8 | Variations in water quality within the CL-DI pipe system. Inset shows the changes in NO_2^- -N concentration with time.

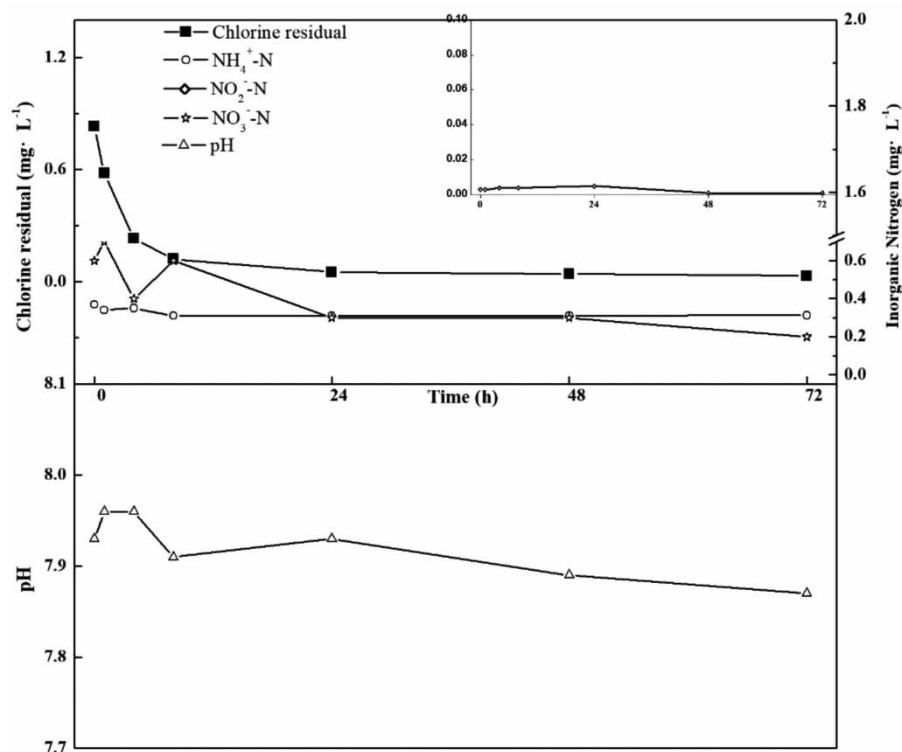


Figure 9 | Variations in water quality within the PPR pipe system. Inset shows the changes in NO₂⁻-N concentration with time.

The biofilm containing AOB and NOB could produce and release some amounts of CDPs (Herath & Sathasivan 2020), zero-valent iron exposed to bulk water can participate in electrochemical corrosion reactions to consume HClO/NH₂Cl and other oxidants. Lime and gypsum leaching caused by flushing can severely reduce NH₄⁺-N to the low level, and further change disinfection chemistry. Here we found that CI, CL-DI, and steel pipes with long service age were characterized by one or two factors driving TCR decay with coordinated variations in water quality. Consequently, with the help of the delivery path information, it is feasible to conduct the analysis on variations in three forms of inorganic nitrogen, pH, and iron residual to confirm the reasons leading to TCR loss, and further take suitable action, e.g., pipeline cleaning, pipeline replacement, etc.

CONCLUSIONS

A new type PSR was operated in continuous flow to study the impact of five pipes on disinfection chemistry. The

contributions of pipe wall to the TCR loss was precisely quantified using refined TCDM (RTCDM). The key conclusions are:

1. The refined TCDM, including the chlorine autodecomposition model, had better performance on predicting TCR decay in the bulk phase, compared with the previous prediction models. Therefore, it is promising to apply the RTCDM to TCR prediction of pipeline water in the future.
2. The PSR could magnify the impact of pipe wall on TCR decay under controlled conditions. For the four typical pipes studied here, the ability of deteriorating water quality, especially for accelerating TCR decay was in the order CI pipe > steel pipe > CL-DI pipe > PPR pipe.
3. CI, CL-DI, and steel pipes with long service age were characterized by one or two driving forces leading to TCR decay. Electrochemical corrosion and nitrification are the main causes for aged CI pipes. Aggressive electrochemical corrosion and weak nitrification are the main causes for aged steel pipes. Lime and gypsum leaching is the main cause, and nitrification/denitrification may

also occur in aged CL-DI pipes. PPR pipes have a minimum effect on disinfection chemistry.

ACKNOWLEDGEMENT

The authors acknowledge the funding offered by Tianjin Water Group Co. Ltd (Project Number: 2019KY-02) and China Postdoctoral Science Foundation (Project Number: 2020M670,671). The authors would like to acknowledge PE. Fushou Wan of Tianjin Hongyuan Water Treatment Engineering Co. Ltd. for his help in providing us with insight into hydrodynamics. The authors also acknowledge Vice Manager Feng Xiao of Lingzhuang Water Treatment Plant in Tianjin for his help in providing the treated water.

DATA AVAILABILITY STATEMENT

All relevant data are included in the paper or its Supplementary Information.

REFERENCES

- Adam, L. C. & Gordon, G. 1998 Hypochlorite ion decomposition: effects of temperature, ionic strength, and chloride ion. *Inorganic Chemistry* **38** (6), 1299–1304.
- Adam, L. C., Fabian, I., Suzuki, K. & Gordon, G. 1992 Hypochlorous acid decomposition in the pH 5-8 region. *Inorganic Chemistry* **31** (17), 3534–3541.
- Church, J. A. 1994 Kinetics of the uncatalyzed and copper(II)-catalyzed decomposition of sodium hypochlorite. *Industrial & Engineering Chemistry Research* **33** (2), 239–245.
- Corbett, R. E., Metcalf, W. S. & Soper, F. G. 1953 Studies of N-halogeno-compounds. Part IV. The reaction between ammonia and chlorine in aqueous solution, and the hydrolysis constants of chloroamines. *Journal of the Chemical Society* **1953**, 1927–1929.
- Dean, J. A. 1985 *Lange's Handbook of Chemistry*. McGraw-Hill, New York.
- Digiano, F. A. & Zhang, W. 2005 Pipe section reactor to evaluate chlorine-wall reaction. *Journal of the American Water Works Association* **97** (1), 74–85.
- Douglas, B. D., Merrill, D. T. & Catlin, J. O. 1996 Water quality deterioration from corrosion of cement-mortar linings. *Journal of the American Water Works Association* **88** (7), 99–107.
- Duirk, S. E., Gombert, B., Croué, J. P. & Valentine, R. L. 2005 Modeling monochloramine loss in the presence of natural organic matter. *Water Research* **39** (14), 3418–3431.
- Fish, K., Osborn, A. M. & Boxall, J. B. 2017 Biofilm structures (EPS and bacterial communities) in drinking water distribution systems are conditioned by hydraulics and influence discolouration. *Science of the Total Environment* **593–594**, 571–580.
- Herath, B. S. & Sathasivan, A. 2020 The chloramine stress induces the production of chloramine decaying proteins by microbes in biomass (biofilm). *Chemosphere* **238**, 124526.
- Hua, G., Baggett, C., Hall, J., Powell, R., Reed, T., Friedrich, T. & Stasis, P. 2011 Controlling nitrification in a distribution system receiving blended multiple source waters: the experience of Pinellas County utilities. *Florida Water Resources Journal* **63** (12), 42–48.
- Huang, X. C. 2008 Reactions between aqueous chlorine and ammonia: a predictive model. Northeastern University: Boston, 2008, 34–42.
- Huang, J. J. & McBean, E. A. 2008 Using Bayesian statistics to estimate chlorine wall decay coefficients for water supply system. *Journal of Water Resources Planning and Management* **134** (2), 129–137.
- Imran, S. A., Dietz, J. D., Mutoti, G., Taylor, J. S., Randall, A. A. & Cooper, C. D. 2005 Red water release in drinking water distribution systems. *Journal of the American Water Works Association* **97** (9), 93–100.
- Janice, S. 1993 Nitrification in a distribution system. *Journal of the American Water Works Association* **85** (7), 95–103.
- Krishna, K. C. B., Sathasivan, A. & Sarker, D. C. 2012 Evidence of soluble microbial products accelerating chloramine decay in nitrifying bulk water samples. *Water Research* **46** (13), 3977–3988.
- Kulkarni, V., Awad, J., van Leeuwen, J., Drikas, M., Chow, C., Cook, D., Medlock, A., Trolino, R. & Amal, R. 2018 Impact of zinc on biologically mediated monochloramine decay in waters from a field based pilot scale drinking water distribution system. *Chemical Engineering Journal* **339**, 240–248.
- Lechevallier, M. W., Cawthon, C. D. & Lee, R. G. 1988 Factors promoting survival of bacteria in chlorinated water supplies. *Applied and Environmental Microbiology* **54** (3), 649–654.
- Lewandowski, Z. & Beyenal, H. 2005 Biofilms: their structure, activity, and effect on membrane filtration. *Water Science and Technology* **51** (6–7), 181–192.
- Li, X., Wang, H., Zhang, Y., Hu, C. & Yang, M. 2014 Characterization of the bacterial communities and iron corrosion scales in drinking groundwater distribution systems with chlorine/chloramine. *International Biodeterioration and Biodegradation* **96**, 71–79.
- Liu, X., Liu, H. & Ding, N. 2020 Chloramine disinfection-induced nitrification activities and their potential public health risk indications within deposits of a drinking water supply system. *International Journal of Environmental Research and Public Health* **17** (3), 772.

- Ma, K., Hu, J., Han, H., Zhao, L., Li, R. & Su, X. 2020 [Characters of chloramine decay in large looped water distribution system – the case of Tianjin, China](#). *Water Supply* **20** (4), 1474–1483.
- Margerum, D. W., Schurter, L. M., Hobson, J. L. & Moore, E. E. 1994 [Water chlorination chemistry: nonmetal redox kinetics of chloramine and nitrite ion](#). *Environmental Science and Technology* **28** (2), 331–337.
- Morris, J. C. & Isaac, R. 1983 Critical review of kinetic and thermodynamic constants for the aqueous chlorine-ammonia system. *Water Chlorination* **4**, 49–62.
- Neden, D. G., Jones, R. J., Smith, J. R., Kirmeyer, G. J. & Foust, G. W. 1992 [Comparing chlorination and chloramination for controlling bacterial regrowth](#). *Journal-American Water Works Association* **84** (7), 80–88.
- Pan, Y., Ye, L., Ni, B.-J. & Yuan, Z. 2012 [Effect of pH on N₂O reduction and accumulation during denitrification by methanol utilizing denitrifiers](#). *Water Research* **46** (15), 4832–4840.
- Peng, Y. Z., Shao-Po, W., Shu-Ying, W., Jian-Ge, H. & Hai-Bing, Q. 2006 [Effect of denitrification type on pH profiles in the sequencing batch reactor process](#). *Water Science and Technology* **53** (9), 87–93.
- Pisigan Jr., R. A. & Singley, J. E. 1985 [Effects of water quality parameters on the corrosion of galvanized steel](#). *Journal of the American Water Works Association* **77** (11), 76–82.
- Pressman, J. G., Lee, W. H., Bishop, P. L. & Wahman, D. G. 2012 [Effect of free ammonia concentration on monochloramine penetration within a nitrifying biofilm and its effect on activity, viability, and recovery](#). *Water Research* **46** (3), 882–894.
- Ricca, H., Aravinthan, V. & Mahinthakumar, G. 2019 [Modeling chloramine decay in full-scale drinking water supply systems](#). *Water Environment Research* **91** (5), 441–454.
- Rittmann, B. E., Huck, P. M. & Bouwer, E. J. 1989 Biological treatment of public water supplies. *Critical Reviews in Environmental Science and Technology* **19** (2), 119–184.
- Rossmann, L. A., Clark, R. M. & Grayman, W. M. 1994 [Modeling chlorine residuals in drinking-water distribution systems](#). *Journal of Environmental Engineering* **120** (4), 803–820.
- Vikesland, P. J., Ozekin, K. & Valentine, R. L. 2001 [Monochloramine decay in model and distribution system waters](#). *Water Research* **35** (7), 1766–1776.
- Wahman, D. G. 2018 [Web-Based applications to simulate drinking water inorganic chloramine chemistry](#). *Journal of the American Water Works Association* **110** (11), E43–E61.
- Westbrook, A. & Digiano, F. A. 2009 [Rate of chloramine decay at pipe surfaces](#). *Journal of the American Water Works Association* **101** (7), 59–70.
- Woolschlager, J. E., Rittmann, B. E. & Piriou, P. 2005 [Water quality decay in distribution systems – problems, causes, and new modeling tools](#). *Urban Water Journal* **2** (2), 69–79.
- Zhang, Y., Triantafyllidou, S. & Edwards, M. 2008 [Effect of nitrification and GAC filtration on copper and lead leaching in home plumbing systems](#). *Journal of Environmental Engineering* **134** (7), 521–530.
- Zhang, Y., Love, N. & Edwards, M. 2009 [Nitrification in drinking water systems](#). *Critical Reviews in Environmental Science and Technology* **39** (3), 153–208.
- Zhang, L., Liu, S. & Liu, W. 2014 [Investigation of organic matter migrating from polymeric pipes into drinking water under different flow manners](#). *Environmental Science Processes and Impacts* **16** (2), 280.
- Zhang, C., Li, C., Zheng, X., Zhao, J., He, G. & Zhang, T. 2017 [Effect of pipe materials on chlorine decay, trihalomethanes formation, and bacterial communities in pilot-scale water distribution systems](#). *International Journal of Environmental Science and Technology* **14** (1), 85–94.

First received 15 October 2020; accepted in revised form 10 December 2020. Available online 21 December 2020